Supporting Information

Enhancing Fluorescent Probe Design Through Multilayer Interaction Convolutional Networks: Advancing Biosensing and Bioimaging Precision

Gongcheng Ma,[a]‡ Qihang Ding,[c]‡* Yuding Zhang,[d]‡ Xiaodong Zeng,[g,h]‡ Kai Zhu,[b] Hongli Chen,[a] Wenxuan Zhang,[e] Qingzhi Wang,[a] Shuman Huang,[b] Ping Gong,[d]* Zhengwei Xu,[b]* and Xuechuan Hong[f,g,h]*

[a]School of Life Science and Technology, Xinxiang Medical University, Xinxiang, 453003, China.
[b]Key Laboratory of Artificial Intelligence and Personalized Learning in Education of Henan Province, School of Computer and Information Engineering, Henan Normal University, Xinxiang, 453007, China.
[c]Department of Chemistry, Korea University, Seoul 02841, Korea
[d]Guangdong Key Laboratory of Nanomedicine, CAS-HK Joint Lab of Biomaterials, CAS Key Laboratory of Biomedical Imaging Science and System, Shenzhen Engineering Laboratory of Nanomedicine and Nanoformulations, CAS Key Lab for Health Informatics, Shenzhen Institutes of Advanced Technology, Chinese Academy of Sciences, Shenzhen 518055, China.
[e]Institute of Materia Medica, Chinese Academy of Medical Sciences and Peking Union Medical College, Beijing, 100050, China.
[f]Department of Cardiology, Zhongnan Hospital of Wuhan University, School of Pharmaceutical Sciences, Wuhan University, Wuhan, 430071, China
[g]State Key Laboratory of Drug Research, Shanghai Institute of Materia Medica, Chinese Academy of Sciences, Shanghai, 201203, China
[h]Shandong Laboratory of Yantai Drug Discovery, Bohai Rim Advanced Research Institute for Drug Discovery, Yantai, 264117, China
[*]Corresponding authors: xhy78@whu.edu.cn (X. Hong); dingqihang@whu.edu.cn (Q. Ding); ping.gong@siat.ac.cn (P. Gong); xuzhengweihhu@outlook.com (Z. Xu)
[‡]These authors contributed equally to this work

MATERIALS AND METHODS

Experimental Procedures

Materials and reagents. Rh640 perchlorate was purchased from Alpha Chemical. Rh19, RhB and Rh110 were purchased from Aladdin Biochemical Technology. Diethylenetriamine was purchased from Alfa Chemical. Dimethylformamide, methanol, dichloromethane and other organic reagents was purchased from Energy-chemical.

Rhodamine probe data collection. The dataset was gathered from the literature, as listed in the Supporting Information (SI). There were in total 610 rhodamine molecules (After filtering) collected from published works. If multiple peaks were seen for the same compound in the same solvent, the peak with the longest wavelength/largest intensity was collected for the absorption data.

Transforming probe structure into computer-recognizable fingerprints. The collected probe structures are converted into recognizable SMILES machine codes based on the ChemDraw. The SMILES machine codes are then input for molecular descriptors and fingerprints, which are derived from the open-source tool ChemDes (http://www.scbdd.com/chemdes) to get the final computer recognizable RDKit descriptor. Morgan fingerprints and MACCSKeys fingerprints are obtained from RDKit (http://www.rdkit.org). There are no quantum mechanical calculations, and these data processing methods are based on high-throughput calculations. After removing some unrecognizable and unsuccessful molecules, the final database contains a total of 614 samples.

Network construction

VGG network architecture: The VGG network architecture is a convolutional neural network, that employs numerous comparatively modest convolutional kernels in a multi-layered configuration to facilitate the extraction of image features. However, one of the VGG architecture's shortcomings is that it is susceptible to overfitting due to a lack of regularisation techniques employed to counteract this phenomenon. Furthermore, the VGG network architecture necessitates a lengthy training period due to the necessity of parameter initialization and optimization for each convolution layer.

ResNet network architecture: The ResNet network architecture is a deep residual network, which is primarily distinguished by the utilisation of jump connections to address the issue of gradient disappearance in deep networks. Nevertheless, the ResNet network architecture is also characterised by a significant computational burden, as it necessitates the initialisation and optimisation of the parameters of each residual block. Furthermore, the ResNet network architecture requires a considerable amount of time for training, due to the necessity of multiple forward and backward propagation for each residual block.

CNN-LSTM network architecture: CNN-LSTM network architecture is a deep learning model based on causal inference, which is characterized by the use of causal inference to solve the uncertainty in forecasting problems. However, the disadvantage of CNN-LSTM network architecture is that it takes a long time to train because it requires multiple reasoning and post-processing for each sample. In addition, the CNN-LSTM network architecture is less interpretable because it uses complex causal inference algorithms.

VATTL algorithm: The VATTL algorithm is a deep learning model based on a self-attention mechanism, which is mainly characterized by the use of a self-attention mechanism to extract important information from input sequences. However, the disadvantage of the VATTL algorithm is that it takes a long time to train because it requires multiple self-attention calculations and post-processing for each sample. In addition, the VATTL algorithm is less interpretable because it uses a complex self-attention mechanism.

MRE (Mean Relative Error): MRE is the average relative error between predicted and actual values (relative error refers to the ratio of error to true value). MRE can reflect the relative error size, but cannot reflect the absolute error size.

$$\text{MRE} = \frac{1}{n}\sum_{i=1}^{n}\left|\frac{y_i - \hat{y}_i}{y_i}\right|,$$

n is the number of samples, y_i is the true value, and $\hat{y}_i$ is the predicted value.

MAE (Mean Absolute Error): MAE is the average absolute difference between all predicted values and the true value, directly reflecting the average difference between the predicted value and the true value.

$$\text{MAE} = \frac{1}{n}\sum_{i=1}^{n}\left|y_i - \hat{y}_i\right|,$$

n is the number of samples, y_i is the true value, and $\hat{y}_i$ is the predicted value.

MSE (Mean Squared Error): MSE is the average of the squared differences between predicted and actual values, used to measure the prediction error of a model. The smaller the MSE, the better the prediction performance of the model.

$$\text{MSE} = \frac{1}{n}\sum_{i=1}^{n}(y_i - \hat{y}_i)^2,$$

n is the number of samples, y_i is the true value, and $\hat{y}_i$ is the predicted value.

RMSE (Root Mean Square Error): RMSE measures the degree of deviation between predicted and true values. The smaller the value, the smaller the prediction error of the model and the stronger its predictive ability.

$$\text{RMSE} = \sqrt{\frac{1}{n}\sum_{i=1}^{n}(y_i - \hat{y}_i)^2},$$

n is the number of samples, y_i is the true value, and $\hat{y}_i$ is the predicted value.

The synthesis of Rh640-N-NH_2, Rh110-N-NH_2, Rh19-N-NH_2 and RhB-N-NH_2: Rhodamine 640 perchlorate (59.10 mg, 0.100 mmol) was dissolved in 10 mL of DMF, and 1-Ethyl-3-(3-dimethylaminopropyl) carbodiimide (EDC) (18.75 mg, 0.150 mmol) was added under stirring at room temperature under a nitrogen atmosphere for 30 minutes. Subsequently, N-(2-aminoethyl) ethane-1,2-diamine hydrochloride (13.96 mg, 0.100 mmol) was added to the mixture, and the reaction mixture was stirred overnight. After solvent removal, purification was performed on silica gel using CH_2Cl_2/MeOH (v/v, 5:1) as eluent, followed by drying under vacuum to yield a red solid Rh640-N-NH_2 (26.59 mg, 36.59%). $[M+H]^+$ = 577.39 (calcd for $C_{36}H_{42}N_5O_2$: 576.33). Based on the same process mentioned above, Rh110-N-NH_2, Rh19-N-NH_2, and RhB-N-NH_2 can be obtained. Yellow solid Rh110-N-NH_2 (31.05 mg, 38.73%). $[M+H]^+$= 417.27 (calcd for $C_{24}H_{26}N_5O_2$: 416.21). Yellow solid Rh19-N-NH_2 (29.40 mg, 32.03%). $[M+H]^+$= 473.33 (calcd for $C_{28}H_{34}N_5O_2$: 472.27). Pink solid RhB-N-NH_2 (15.64 mg, 26.84%). $[M+H]^+$= 529.39 (calcd for $C_{32}H_{42}N_5O_2$: 528.33).

The synthesis of Rh640-fluorescein, Rh110-fluorescein, Rh19-fluorescein and RhB-fluorescein.

In anhydrous DMF, a mixture of fluorescein (33.11 mg, 0.100 mmol), EDC (18.75 mg, 0.150 mmol), and 4-(Dimethylamino) pyridine (DMAP) (18.33 mg, 0.150 mmol) was stirred under a nitrogen atmosphere at room temperature for 30 minutes. The prepared Rh640-N-NH_2 (57.63 mg, 0.100 mmol) was added, and the reaction was stirred overnight. After solvent removal, purification was carried out on silica gel using CH_2Cl_2/MeOH (v/v, 15:1) as eluent, resulting in the isolation of an orange solid Rh640-fluorescein (10.06 mg, 11.09%). $[M+H]^+$= 891.45 (calculated for $C_{56}H_{52}N_5O_6$: 890.39). Based on the same process mentioned above, Rh110-fluorescein, Rh19-fluorescein, and RhB-fluorescein can be obtained. Yellow solid Rh110-fluorescein (16.50 mg, 22.08%). $[M+H]^+$= 731.33 (calcd for $C_{44}H_{36}N_5O_6$: 730.27). Yellow solid Rh19-fluorescein (10.63 mg, 13.68%) $[M+H]^+$= 787.39 (calcd for $C_{48}H_{44}N_5O_6$: 786.33). Orange solid RhB-fluorescein (11.84 mg, 14.74%), $[M+H]^+$= 843.45 (calcd for $C_{52}H_{52}N_5O_6$: 842.39).

Figures

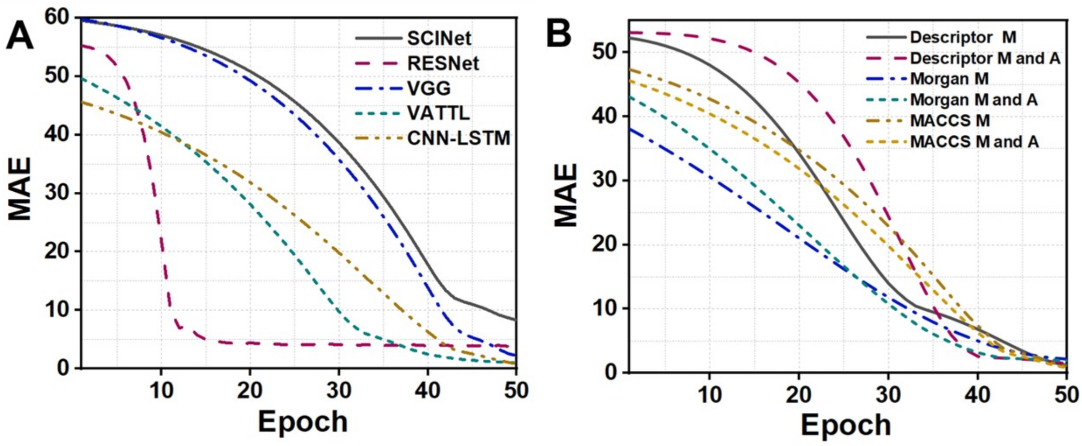

Figure S1. The predicted maximum excitation values plotted against observed data in 20-fold cross-validation, respectively. Three feature acquisition methods including RDKit descriptors, Morgan fingerprints, MACCSKeys fingerprints were applied, followed by employed MICNet and four compare methods, namely CNN-LSTM, RESNet VGG and VATTL.

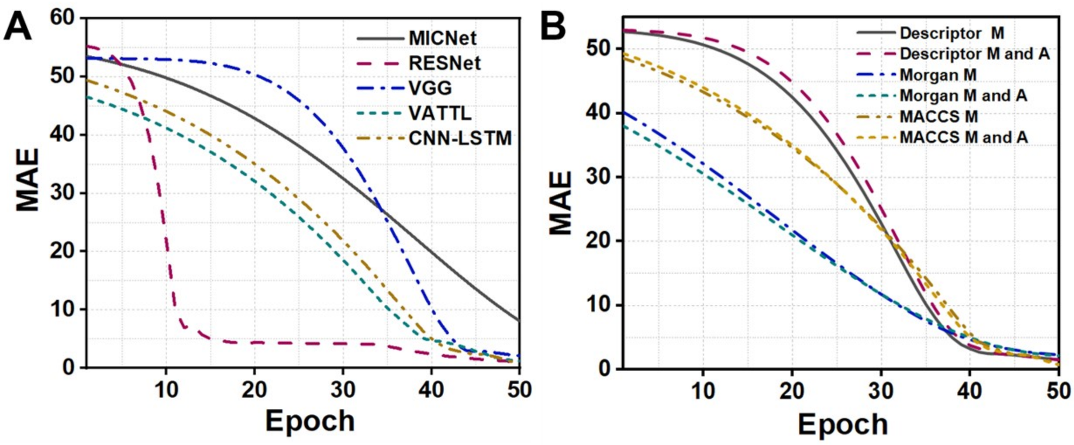

Figure S2. The predicted maximum emission values plotted against observed data in 20-fold cross-validation, respectively. Three feature acquisition methods including RDKit descriptors, Morgan fingerprints, MACCSKeys fingerprints were applied, followed by employed MICNet and four compare methods, namely CNN-LSTM, RESNet, VGG and VATTL.

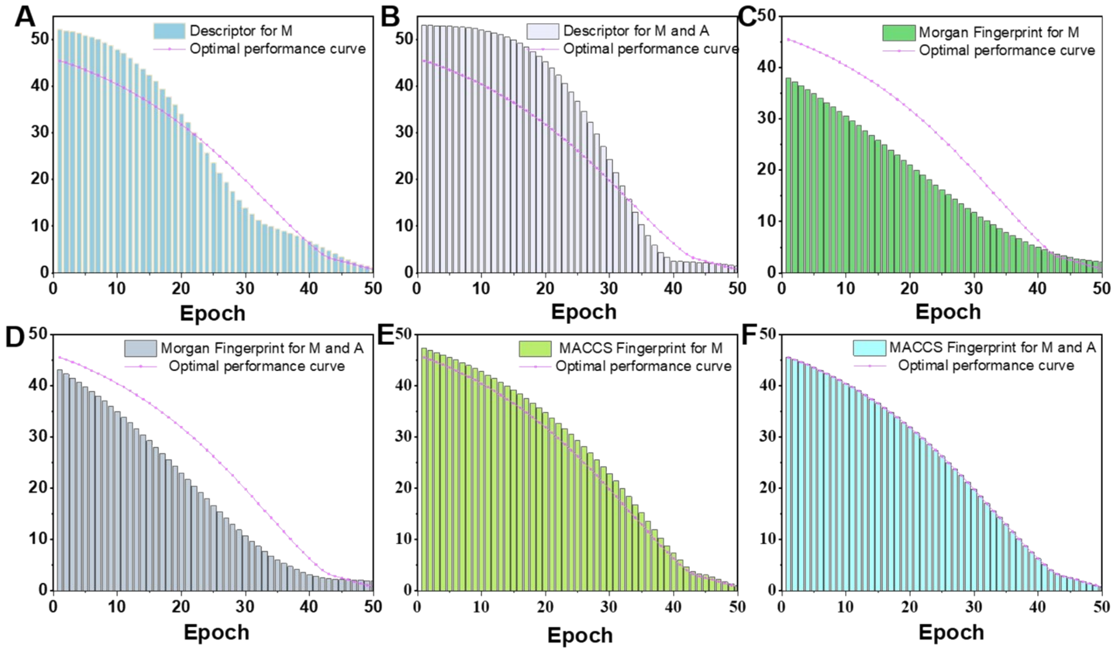

Figure S3. The predicted maximum excitation values plotted against observed data in 20-fold cross-validation. Three feature acquisition methods including RDKit descriptors, Morgan fingerprints, MACCSKeys fingerprints were applied, followed by employed MICNet.

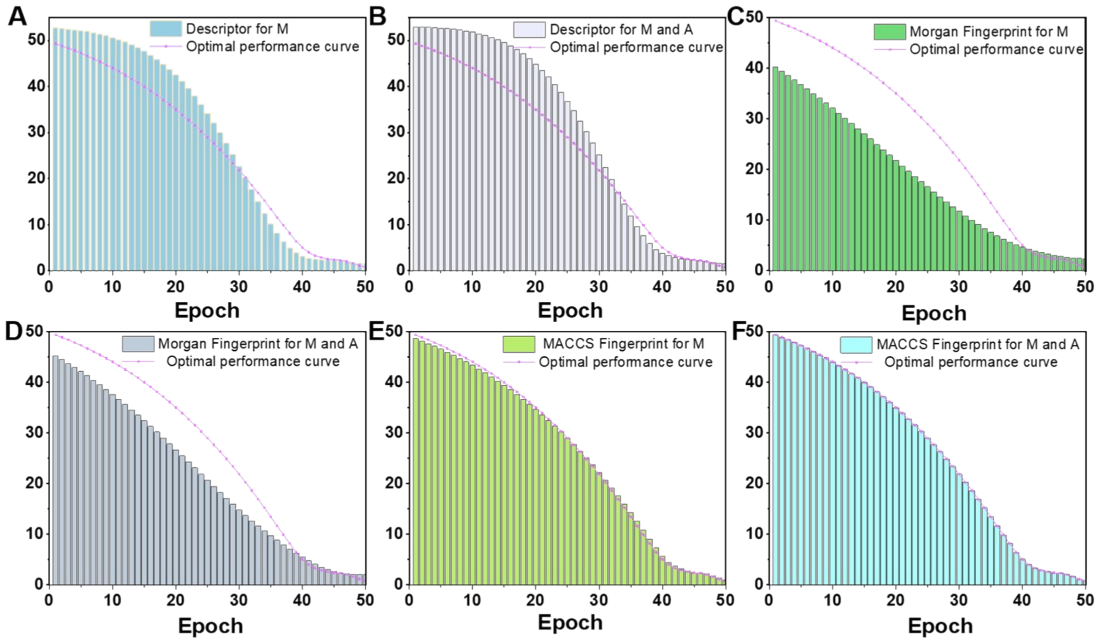

Figure S4. The predicted maximum emission values plotted against observed data in 20-fold cross-validation. Three feature acquisition methods including RDKit descriptors, Morgan fingerprints, MACCSKeys fingerprints were applied, followed by employed MICNet.

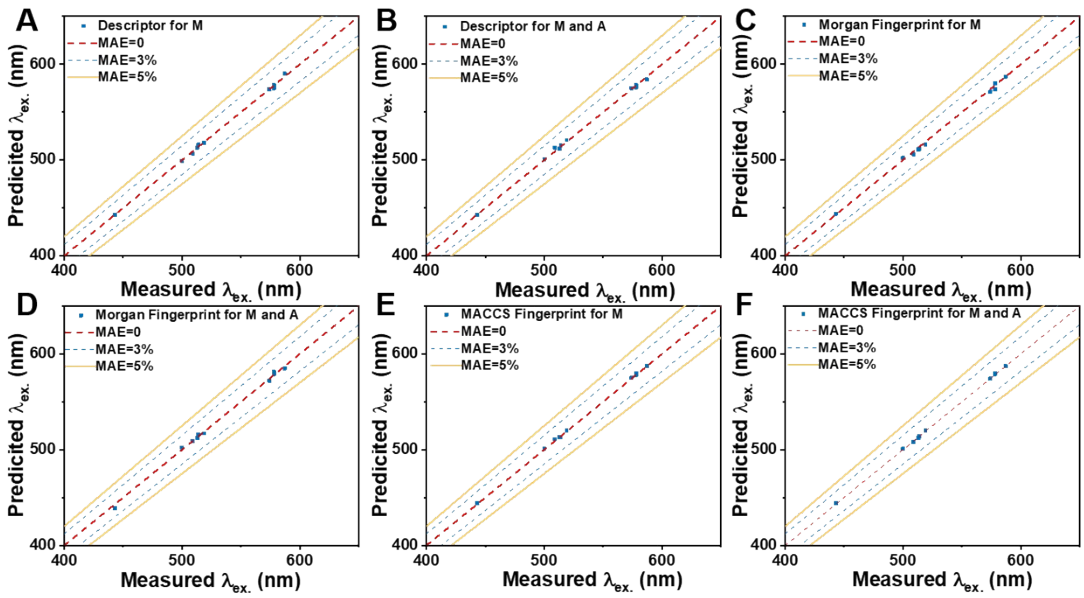

Figure S5. The point-line distribution map of the excitation values of test probe. Three feature acquisition methods including RDKit descriptors, Morgan fingerprints, MACCSKeys fingerprints were applied, followed by employed MICNet. (MAE range: 0, 3% and 5%)

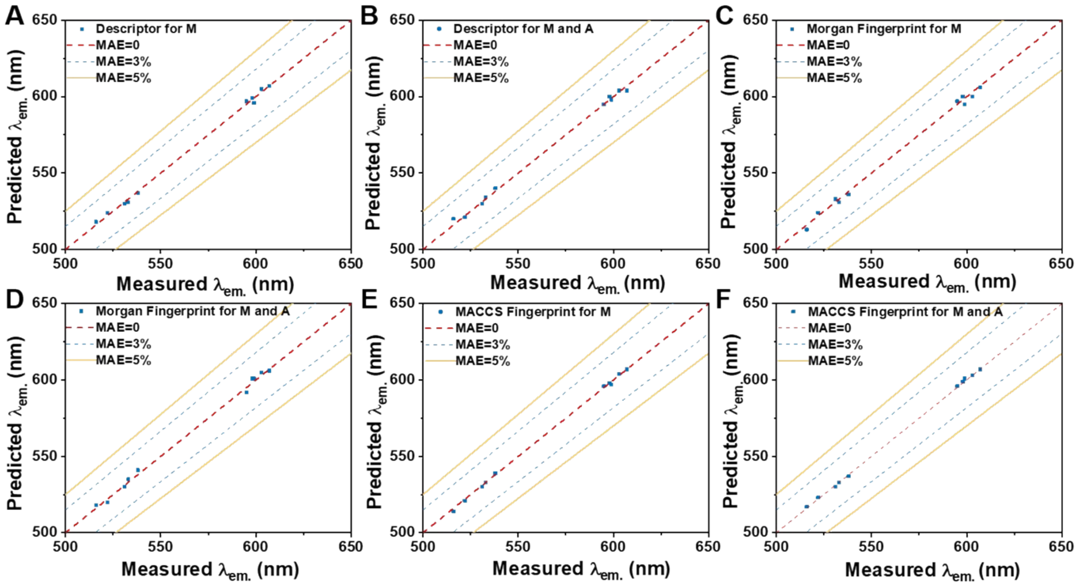

Figure S6. The point-line distribution map of the emission values of test probe. Three feature acquisition methods including RDKit descriptors, Morgan fingerprints, MACCSKeys fingerprints were applied, followed by employed MICNet. (MAE range: 0, 3% and 5%)

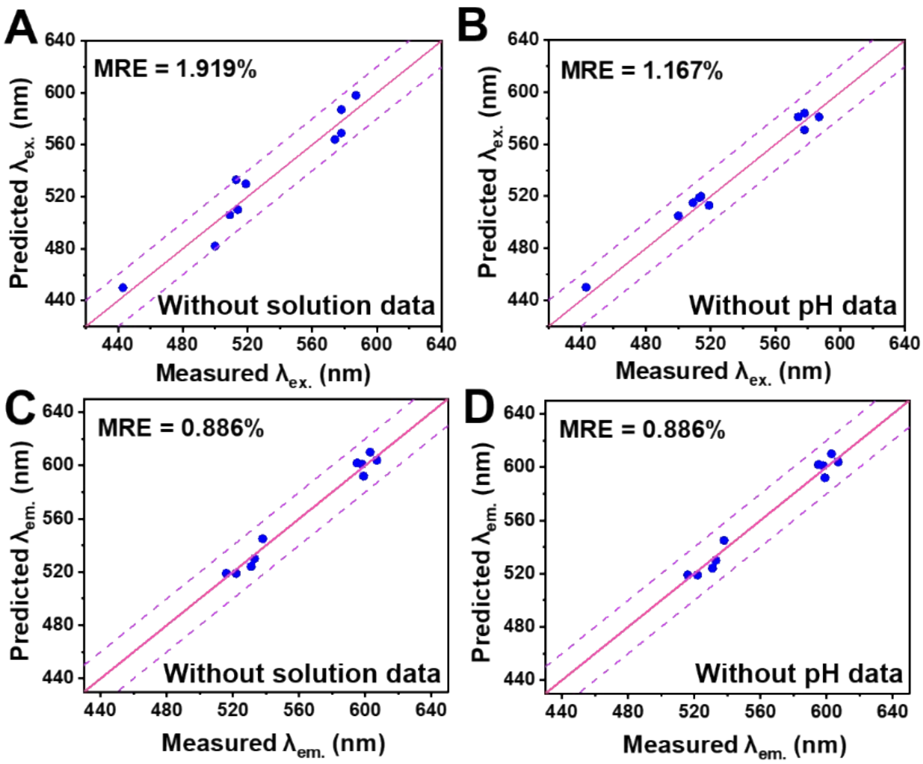

Figure S7. The point-line distribution map of the excition and emission values of test probe without solution data or pH data. Three feature acquisition methods including RDKit descriptors, Morgan fingerprints, MACCSKeys fingerprints were applied, followed by employed MICNet. (MRE range: 0 and 3%)

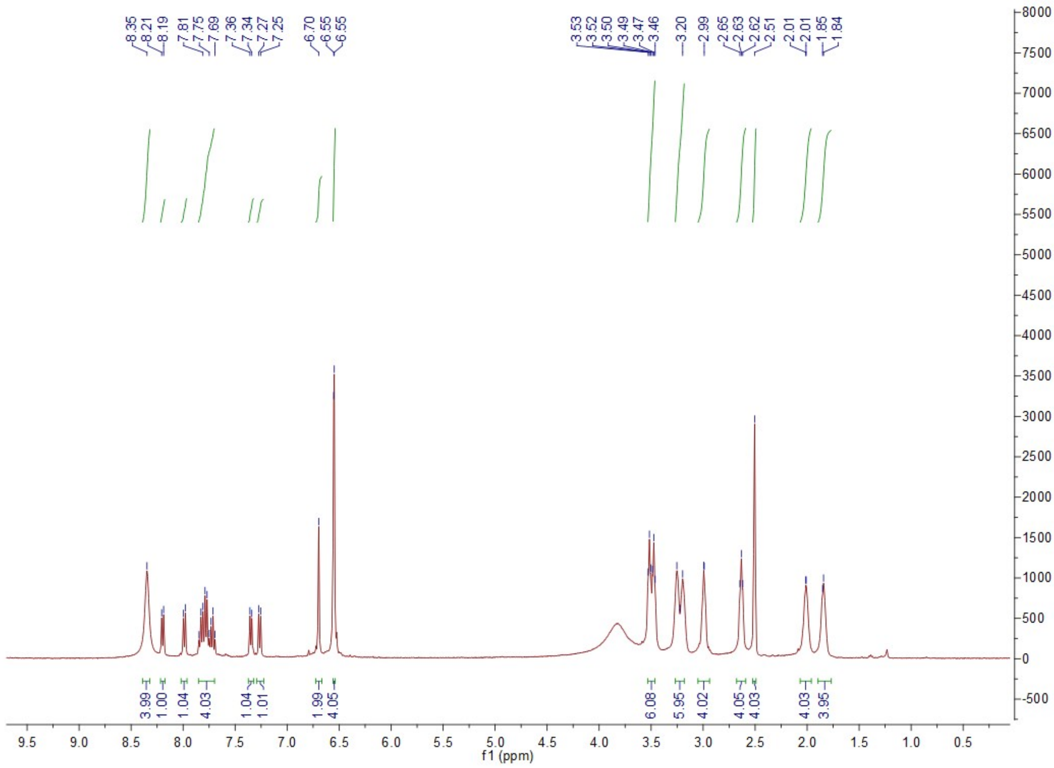

Figure S8. The HNMR spectrum of Rh640-Fluorescein.

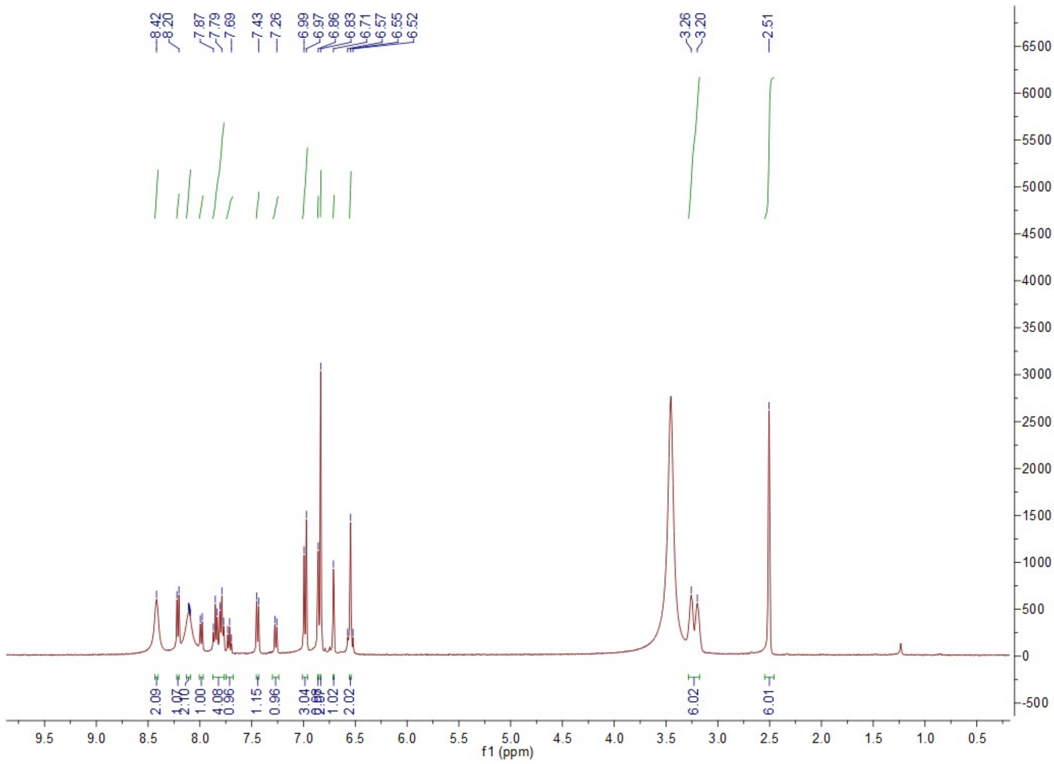

Figure S9. The HNMR spectrum of Rh110-Fluorescein.

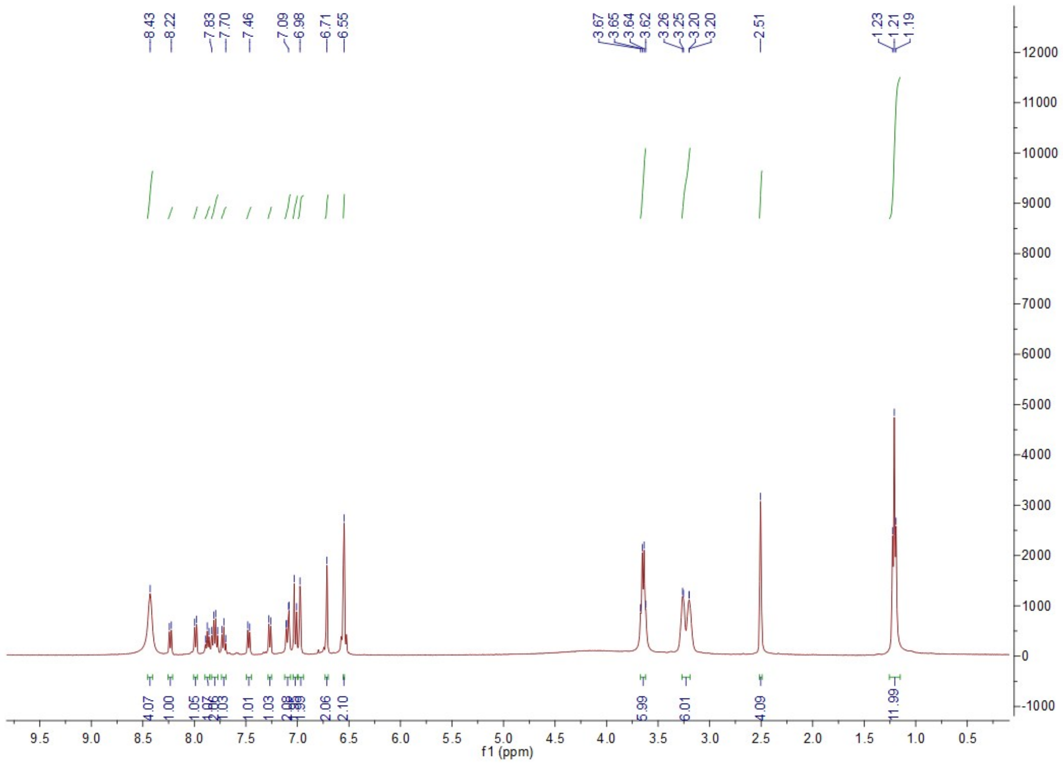

Figure S10. The HNMR spectrum of RhB-Fluorescein.

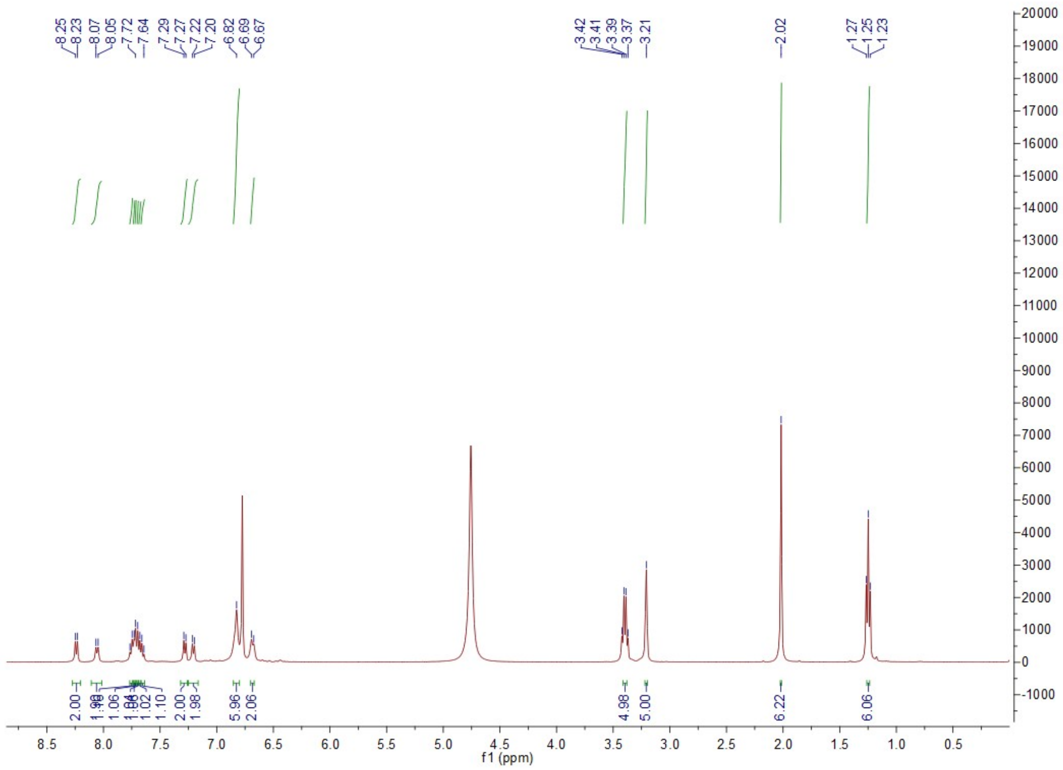

Figure S11. The HNMR spectrum of Rh19-Fluorescein.

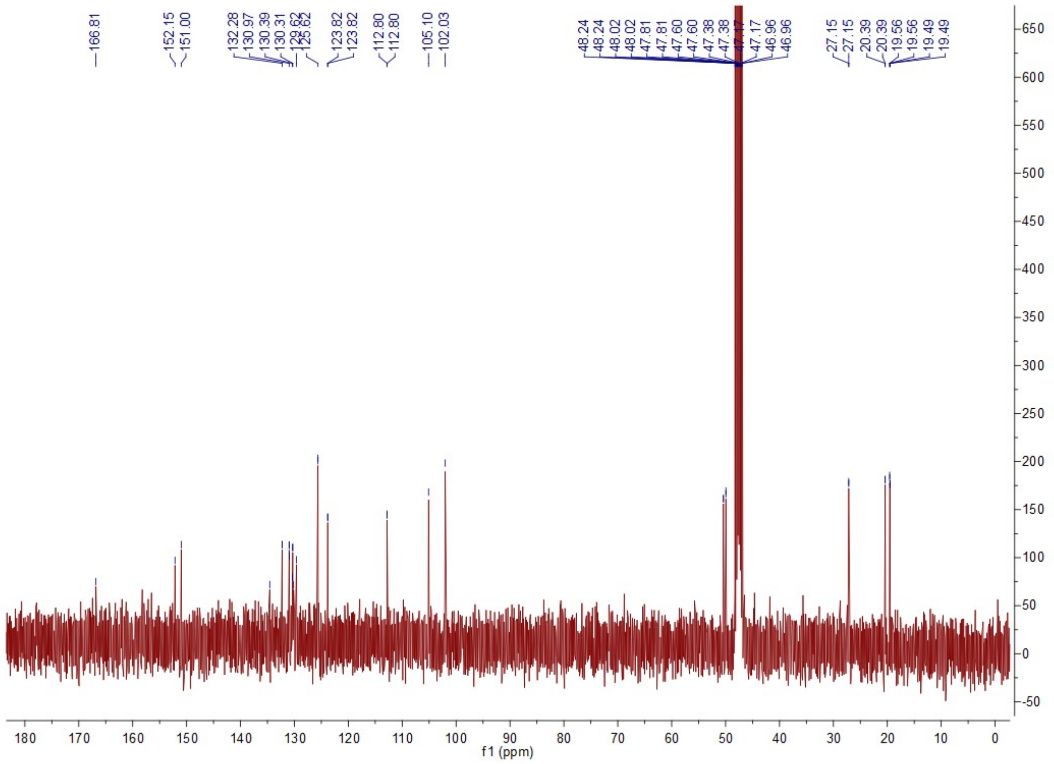

Figure S12. The CNMR spectrum of Rh640-Fluorescein.

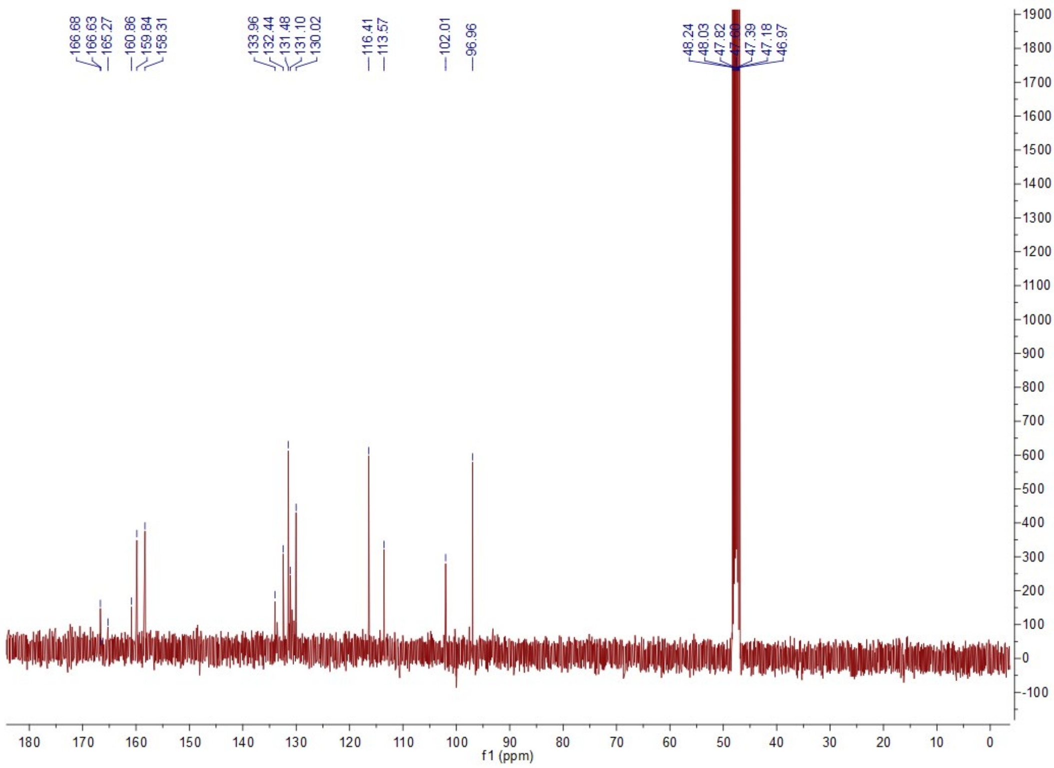

Figure S13. The CNMR spectrum of Rh110-Fluorescein.

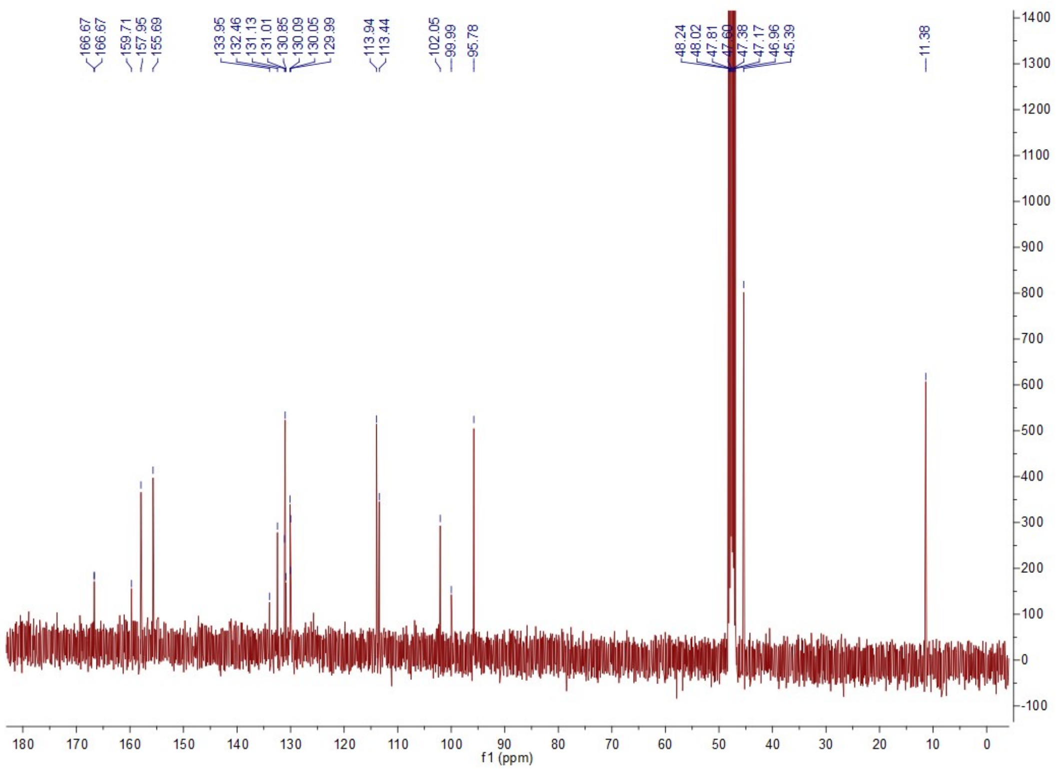

Figure S14. The CNMR spectrum of RhB-Fluorescein.

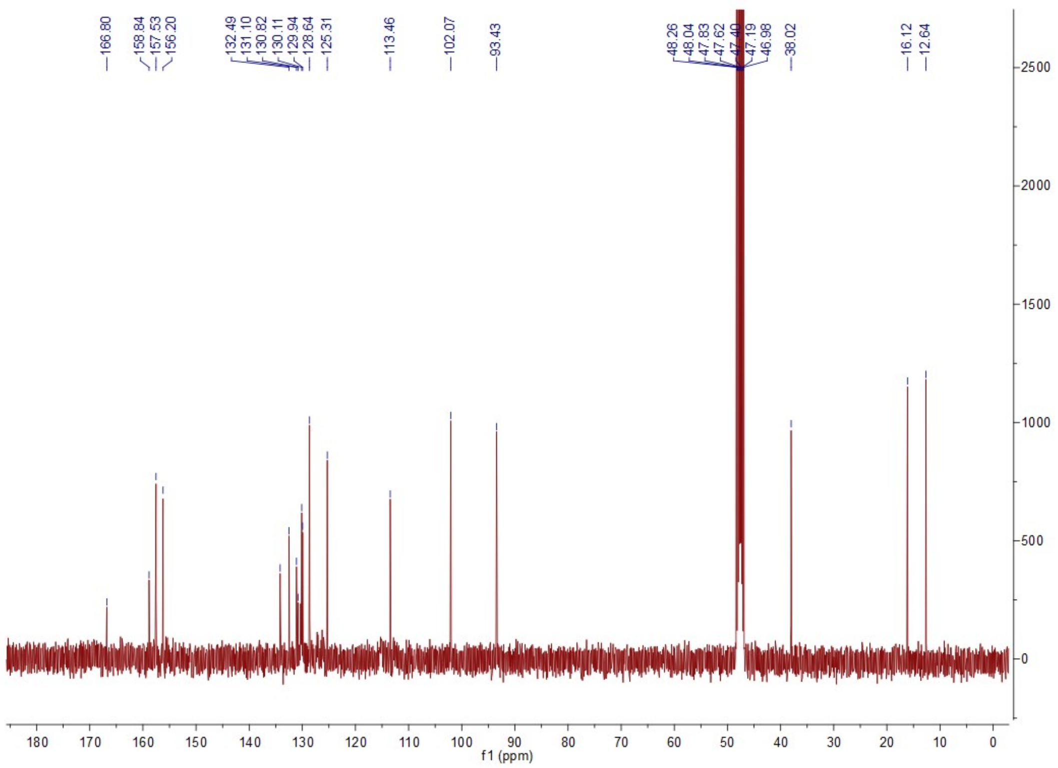

Figure S15. The CNMR spectrum of Rh19-Fluorescein.

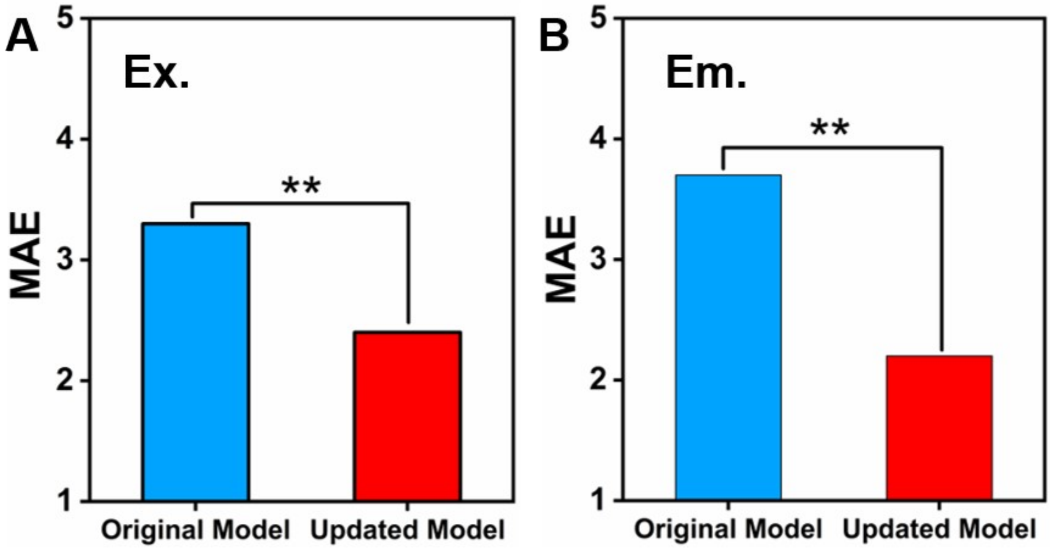

Figure S16. The P value in predicting the excitation (A) and the emission (B) of the test probe before and after database updates. (*P<0.05, **P<0.005, and ***P<0.0005,n=3).

References for dataset construction

[1] Synthesis and applications of Rhodamine derivatives as fluorescent probes[J]. Chemical Society Reviews, 2009, 38(8): 2410-2433.

[2] Fluorescent dyes based on rhodamine derivatives for bioimaging and therapeutics: recent progress, challenges, and prospects[J]. Chemical Society Reviews, 2023.

[3] Recent Trends in Rhodamine derivatives as fluorescent probes for biomaterial applications[J]. Journal of Molecular Structure, 2021, 1235: 130232.

[4] A recent update on rhodamine dye-based sensor molecules: a review[J]. Critical Reviews in Analytical Chemistry, 2023: 1-27.

[5] A review on rhodamine probes for metal ion recognition with a future on artificial intelligence and machine learning[J]. Coordination Chemistry Reviews, 2023, 495: 215371.

[6] Recent developments in rhodamine-based chemosensors: A review of the years 2018–2022[J]. Chemosensors, 2022, 10(10): 399.

[7] Hybrid rhodamine fluorophores in the visible/NIR region for biological imaging[J]. Angewandte Chemie International Edition, 2019, 58(40): 14026-14043.

[8] Rhodamine-based ratiometric fluorescent probes based on excitation energy transfer mechanisms: construction and applications in ratiometric sensing[J]. Rsc Advances, 2016, 6(56): 50732-50760.

[9] Recent developments in rhodamine salicylidene hydrazone chemosensors[J]. Analytical Methods, 2016, 8(14): 2863-2871.

[10] Teaching old dyes new tricks: biological probes built from fluoresceins and rhodamines[J]. Annual review of biochemistry, 2017, 86(1): 825-843.

[11] Recent progress and outlooks in rhodamine-based fluorescent probes for detection and imaging of reactive oxygen, nitrogen, and sulfur species[J]. Talanta, 2024, 274: 126004.

[12] Design and application of rhodamine derivatives in redox biology: a roadmap of the last

decade towards artificial intelligence[J]. Journal of Materials Chemistry A, 2024.
[13] Design strategies to rhodamine analogue fluorophores for near-infrared II biological imaging applications[J]. Dyes and Pigments, 2021, 196: 109792.
[14] Rhodols–synthesis, photophysical properties and applications as fluorescent probes[J]. Chemical Society Reviews, 2019, 48(20): 5242-5265.
[15] FRET-based small-molecule fluorescent probes: rational design and bioimaging applications[J]. Accounts of chemical research, 2013, 46(7): 1462-1473.
[16] Rhodamine Fluorophores for STED Super‐Resolution Biological Imaging[J]. Analysis & Sensing, 2022, 2(3): e202100066.
[17] Review on Metal Ion Recognition by Bis-Rhodamine Probes with a Future in Artificial Intelligence and Machine Learning[J]. Journal of Molecular Structure, 2024: 137597.
[18] Rhodamine and BODIPY chemodosimeters and chemosensors for the detection of Hg 2+, based on fluorescence enhancement effects[J]. Analytical Methods, 2013, 5(1): 30-49.
[19] Rhodamine B and rhodamine 6G based sensing of copper ions in environmental and biological samples: Recent Progress[J]. Polish Journal of Environmental Studies, 2021, 30(4): 3445.
[20] Photophysical, ion-sensing and biological properties of rhodamine-containing transition metal complexes[J]. Coordination Chemistry Reviews, 2020, 416: 213336.
[21] Recent advances in Si-rhodamine-based fluorescent probes for live-cell imaging[J]. Organic & Biomolecular Chemistry, 2024.
[22] A new trend in rhodamine-based chemosensors: application of spirolactam ring-opening to sensing ions[J]. Chemical Society Reviews, 2008, 37(8): 1465-1472.
[23] A study of small molecule-based rhodamine-derived chemosensors and their implications in environmental and biological systems from 2012 to 2021: latest advancement and future prospects[J]. Journal of Fluorescence, 2024, 34(1): 15-118.
[24] Use of fluorescence probes for detection of reactive nitrogen species: a review[J]. Journal of fluorescence, 2006, 16: 119-139.
[25] A brief review on advances in rhodamine B based chromic materials and their prospects[J]. ACS Applied Electronic Materials, 2022, 4(8): 3749-3771.
[26] Recent progress in the development of fluorescent probes for detection of biothiols[J]. Dyes and Pigments, 2020, 177: 108321.
[27] A review on Rhodamine-based Schiff base derivatives: synthesis and fluorescent chemo-sensors behaviour for detection of Fe3+ and Cu2+ ions[J]. Journal of Coordination Chemistry, 2023, 76(3-4): 371-402.
[28] Rhodamine-based fluorescent probes for cations[J]. Progress in Chemistry, 2012, 24(05): 823.
[29] Advances in the chemistry of small molecule fluorescent probes[J]. Current opinion in chemical biology, 2011, 15(6): 752-759.
[30] Structure–metal ion selectivity of rhodamine-based chemosensors[J]. Chemical Communications, 2023, 59(35): 5174-5200.
[31] Review of current developments in rhodamine derivatives-based photoresponsive chemosensors for ion detection[J]. Inorganic Chemistry Communications, 2024: 112143.
[32] Small-molecule fluorophores and fluorescent probes for bioimaging[J]. Pflügers Archiv-

European Journal of Physiology, 2013, 465: 347-359.
[33] Fluorescent probes for sensing and imaging within specific cellular organelles[J]. Accounts of chemical research, 2016, 49(10): 2115-2126.
[34] Fluorescent probe for mercury ion imaging analysis: Strategies and applications[J]. Chemical Engineering Journal, 2021, 406: 127166.
[35] Advances in modifying fluorescein and rhodamine fluorophores as fluorescent chemosensors[J]. Chemical communications, 2013, 49(5): 429-447.
[36] A minireview of viscosity-sensitive fluorescent probes: design and biological applications[J]. Journal of Materials Chemistry B, 2020, 8(42): 9642-9651.
[37] Spectroscopic probes with changeable π-conjugated systems[J]. Chemical Communications, 2012, 48(70): 8732-8744.
[38] A rhodamine-based fluorescent probe for the detection of lysosomal pH changes in living cells[J]. Sensors and Actuators B: Chemical, 2018, 266: 416-421.
[39] Fluorogenic and cell‐permeable rhodamine dyes for high‐contrast live‐cell protein labeling in bioimaging and biosensing[J]. Angewandte Chemie International Edition, 2023, 62(45): e202307641.
[40] Recent progress in pendant rhodamine-based polymeric sensors for the detection of copper, mercury and iron ions[J]. Journal of Macromolecular Science, Part A, 2021, 58(12): 835-848.
[41] Fluorescent probes for pH and alkali metal ions[J]. Coordination Chemistry Reviews, 2021, 427: 213584.
[42] Fluorescent probes and fluorescence (microscopy) techniques—illuminating biological and biomedical research[J]. Molecules, 2012, 17(12): 14067-14090.
[43] Far-red to near infrared analyte-responsive fluorescent probes based on organic fluorophore platforms for fluorescence imaging[J]. Chemical Society Reviews, 2013, 42(2): 622-661.
[44] Recent advances on iron (III) selective fluorescent probes with possible applications in bioimaging[J]. Molecules, 2019, 24(18): 3267.
[45] Recent progress in the development of near-infrared fluorescent probes for bioimaging applications[J]. Chemical Society Reviews, 2014, 43(1): 16-29.
[46] Combinatorial strategies in fluorescent probe development[J]. Chemical reviews, 2012, 112(8): 4391-4420.
[47] Design strategies for water-soluble small molecular chromogenic and fluorogenic probes[J]. Chemical reviews, 2014, 114(1): 590-659.
[48] Fluorogenic probes for super-resolution microscopy[J]. Organic & biomolecular chemistry, 2019, 17(2): 215-233.
[49] Toxicity of organic fluorophores used in molecular imaging: literature review[J]. Molecular imaging, 2009, 8(6): 7290.2009. 00031.
[50] Fluorescent probes for the simultaneous detection of multiple analytes in biology[J]. Chemical Society Reviews, 2018, 47(1): 195-208.
[51] Fluorescent probes based on rhodamine hydrazides and hydroxamates[J]. The Chemical Record, 2016, 16(1): 124-140.
[52] Fluorescent probes for organelle-targeted bioactive species imaging[J]. Chemical science, 2019, 10(24): 6035-6071.

[53] Fluorescent probes and bioimaging: alkali metals, alkaline earth metals and pH[J]. Chemical Society Reviews, 2015, 44(14): 4619-4644.
[54] Recent progress in fluorescent imaging probes[J]. Sensors, 2015, 15(9): 24374-24396.
[55] Synthetic ratiometric fluorescent probes for detection of ions[J]. Chemical Society Reviews, 2020, 49(1): 143-179.
[56] A new kind of rhodamine-based fluorescence turn-on probe for monitoring ATP in mitochondria[J]. Sensors and Actuators B: Chemical, 2018, 265: 429-434.
[57] Small molecule-based ratiometric fluorescence probes for cations, anions, and biomolecules[J]. Chemical Society Reviews, 2015, 44(13): 4185-4191.
[58] A review: the trend of progress about pH probes in cell application in recent years[J]. Analyst, 2017, 142(1): 30-41.
[59] Small-molecule fluorescent probes for imaging gaseous signaling molecules: current progress and future implications[J]. Chemical Science, 2020, 11(20): 5127-5141.
[60] Fluorescent lipid probes: some properties and applications (a review)[J]. Chemistry and physics of lipids, 2002, 116(1-2): 3-18.
[61] Molecular fluorescent probes for monitoring pH changes in living cells[J]. TrAC Trends in Analytical Chemistry, 2010, 29(9): 1004-1013.
[62] Recent progress in fluorescent probes for bacteria[J]. Chemical Society Reviews, 2021, 50(13): 7725-7744.
[63] Engineering an asymmetric rhodamine dye suitable for develo** ratiometric fluorescent probe[J]. Smart Molecules, 2023, 1(1): e20220002.
[64] An endeavor in the reaction-based approach to fluorescent probes for biorelevant analytes: challenges and achievements[J]. Accounts of chemical research, 2019, 52(9): 2571-2581.
[65] Photophysical processes in single molecule organic fluorescent probes[J]. Chemical Society Reviews, 2014, 43(4): 1057-1075.
[66] Rational design of small molecule fluorescent probes for biological applications[J]. Organic & biomolecular chemistry, 2020, 18(30): 5747-5763.
[67] Heteroatom-substituted rhodamine dyes: Structure and spectroscopic properties[J]. Chinese Chemical Letters, 2019, 30(10): 1667-1681.
[68] Solvatochromic and fluorogenic dyes as environment-sensitive probes: design and biological applications[J]. Accounts of chemical research, 2017, 50(2): 366-375.
[69] Asymmetric rhodamine‐based fluorescent probe for multicolour in vivo imaging[J]. Chemistry–A European Journal, 2016, 22(5): 1696-1703.
[70] Fluorescent probes for bioimaging applications[J]. Current opinion in chemical biology, 2008, 12(5): 515-521.
[71] Synthesis and applications of rhodamine fluorescent dyes[J]. Progress in Chemistry, 2006, 18(0203): 252.
[72] One-step activated fluorescence bioimaging of γ-glutamyltransferase activity in living cancer cells based on chloro-rhodamine probe[J]. Dyes and Pigments, 2022, 199: 109962.
[73] A novel Fe3+ fluorescent probe based on rhodamine derivatives and its application in biological imaging[J]. Journal of Molecular Structure, 2022, 1270: 133979.
[74] Recent progresses in fluorescent probes for detection of polarity[J]. Coordination Chemistry Reviews, 2021, 427: 213582.

[75] An edaravone-guided design of a rhodamine-based turn-on fluorescent probe for detecting hydroxyl radicals in living systems[J]. Analytical chemistry, 2021, 93(42): 14343-14350.
[76] Sensors for detection of the synthetic dye rhodamine in environmental monitoring based on SERS[J]. Micromachines, 2022, 13(11): 1840.
[77] BODIPY-based probes for the fluorescence imaging of biomolecules in living cells[J]. Chemical Society Reviews, 2015, 44(14): 4953-4972.
[78] Multimodality imaging probes: design and challenges[J]. Chemical reviews, 2010, 110(5): 3146-3195.
[79] Developments in fluorescent probes for receptor research[J]. Drug discovery today, 2009, 14(13-14): 706-712.
[80] A fluorescent detection pen for sensitive, specific, and real-time detection of phosgene based on a novel rhodamine probe[J]. Sensors and Actuators B: Chemical, 2023, 376: 132971.
[81] Ratiometric fluorescent nanoprobes for visual detection: Design principles and recent advances-A review[J]. Analytica chimica acta, 2019, 1079: 30-58.
[82] Rhodamine and related substances in food: Recent updates on pretreatment and analysis methods[J]. Food Chemistry, 2024: 140384.
[83] Activatable fluorescent probes for in situ imaging of enzymes[J]. Chemical Society Reviews, 2022, 51(2): 450-463.
[84] Small-molecule two-photon probes for bioimaging applications[J]. Chemical Reviews, 2015, 115(11): 5014-5055.
[85] Motion-induced change in emission (MICE) for develo** fluorescent probes[J]. Chemical Society Reviews, 2017, 46(16): 4833-4844.
[86] Cytometric assessment of mitochondria using fluorescent probes[J]. Cytometry Part A, 2011, 79(6): 405-425.
[87] A Bifunctional Fluorogenic Rhodamine Probe for Proximity‐Induced Bioorthogonal Chemistry[J]. Chemistry–A European Journal, 2017, 23(72): 18216-18224.
[88] Rhodamine B as a mitochondrial probe for measurement and monitoring of mitochondrial membrane potential in drug-sensitive and-resistant cells[J]. Journal of Biochemical and Biophysical Methods, 2003, 57(1): 1-16.
[89] Fluorescent probes to investigate nitric oxide and other reactive nitrogen species in biology (truncated form: fluorescent probes of reactive nitrogen species)[J]. Current opinion in chemical biology, 2010, 14(1): 43-49.
[90] "Turn-on" fluorescent probes based on Rhodamine B/amino acid derivatives for detection of Fe3+ in water[J]. Spectrochimica Acta Part A: Molecular and Biomolecular Spectroscopy, 2021, 247: 119095.
[91] Photoresponse and anisotropy of rhodamine dye intercalated in ordered clay layered films[J]. Journal of Photochemistry and Photobiology C: Photochemistry Reviews, 2007, 8(2): 85-108.
[92] Discerning the chemistry in individual organelles with small‐molecule fluorescent probes[J]. Angewandte Chemie International Edition, 2016, 55(44): 13658-13699.
[93] Facile preparation of a rhodamine B derivative-based fluorescent probe for visual detection of iron ions[J]. ACS omega, 2021, 6(38): 25040-25048.

[94] Activity-based NIR fluorescent probes based on the versatile hemicyanine scaffold: design strategy, biomedical applications, and outlook[J]. Chemical Society Reviews, 2022, 51(5): 1795-1835.
[95] Redox-responsive fluorescent probes with different design strategies[J]. Accounts of Chemical Research, 2015, 48(5): 1358-1368.
[96] Fluorescent probes for the visualization of cell viability[J]. Accounts of Chemical Research, 2019, 52(8): 2147-2157.
[97] Progress on Si-Rhodamine Fluorescent Probes[J]. Journal of East China University of Science and Technology, 2019, 45(6): 845-852.
[98] A substituted‐rhodamine‐based reversible fluorescent probe for in vivo quantification of glutathione[J]. Angewandte Chemie, 2023, 135(12): e202217326.
[99] Fluorescent probes and nanoparticles for intracellular sensing of pH values[J]. Methods and applications in fluorescence, 2014, 2(4): 042001.
[100] Iron (III) selective molecular and supramolecular fluorescent probes[J]. Chemical Society Reviews, 2012, 41(21): 7195-7227.
[101] Design strategy for germanium-rhodamine based pH-activatable near-infrared fluorescence probes suitable for biological applications[J]. Communications Chemistry, 2019, 2(1): 94.
[102] New strategies for fluorescent probe design in medical diagnostic imaging[J]. Chemical reviews, 2010, 110(5): 2620-2640.
[103] Progress in modifications and applications of fluorescent dye probe[J]. Progress in Natural Science, 2009, 19(1): 1-7.
[104] Photophysics of fluorescent probes for single-molecule biophysics and super-resolution imaging[J]. Annual review of physical chemistry, 2012, 63(1): 595-617.
[105] Small molecule as fluorescent probes for monitoring intracellular enzymatic transformations[J]. Chemical reviews, 2019, 119(22): 11718-11760.
[106] Fluorescent probes for super-resolution imaging in living cells[J]. Nature reviews Molecular cell biology, 2008, 9(12): 929-943.
[107] One probe for multiple targets: A NIR fluorescent rhodamine-based probe for $ONOO^-$ and lysosomal pH detection in live cells[J]. Sensors and Actuators B: Chemical, 2021, 337: 129732.
[108] Recent advances in dual-emission ratiometric fluorescence probes for chemo/biosensing and bioimaging of biomarkers[J]. Coordination Chemistry Reviews, 2019, 383: 82-103.
[109] Novel fluorescent probe toward Fe3+ based on rhodamine 6G derivatives and its bioimaging in adult mice, Caenorhabditis elegans, and plant tissues[J]. ACS omega, 2021, 6(12): 8616-8624.
[110] Review on recent advances in metal ions sensing using different fluorescent probes[J]. Journal of fluorescence, 2018, 28: 999-102
[111] Review on recent advances in metal ions sensing using different fluorescent probes[J]. Journal of fluorescence, 2018, 28: 999-1021.
[112] Recent advances in formaldehyde-responsive fluorescent probes[J]. Chinese Chemical Letters, 2017, 28(10): 1935-1942.
[113] Near-infrared fluorescent probes in cancer imaging and therapy: an emerging field[J].

International Journal of nanomedicine, 2014: 1347-1365.
[114] A reversible rhodamine B based pH probe with large pseudo‐Stokes shift[J]. ChemPlusChem, 2019, 84(7): 816-820.
[115] Small molecule based fluorescent chemosensors for imaging the microenvironment within specific cellular regions[J]. Chemical Society Reviews, 2021, 50(21): 12098-12150.
[116] Small molecular fluorescent probes for imaging of viscosity in living biosystems[J]. Chemistry–A European Journal, 2021, 27(23): 6880-6898.
[117] Selenium-and tellurium-containing fluorescent molecular probes for the detection of biologically important analytes[J]. Accounts of chemical research, 2014, 47(10): 2985-2998.
[118] Creating new fluorescent probes for cell biology[J]. Nature reviews Molecular cell biology, 2002, 3(12): 906-918.
[119] A new near-infrared ratiometric fluorescent probe based on quinoline-fused rhodamine dye for sensitive detection of cysteine and homocysteine in mitochondria[J]. Dyes and Pigments, 2020, 183: 108710.
[120] Resonance energy transfer-based fluorescent probes for Hg 2+, Cu 2+ and Fe 2+/Fe 3+ ions[J]. Analyst, 2014, 139(3): 543-558.
[121] Multi-channel detection of Au (III) ions by a novel rhodamine based probe[J]. Sensors and Actuators B: Chemical, 2022, 360: 131658.
[122] Fluorescent and luminescent probes for measurement of oxidative and nitrosative species in cells and tissues: progress, pitfalls, and prospects[J]. Free radical biology and medicine, 2007, 43(7): 995-1022.
[123] Characterization of a Hg2+-selective fluorescent probe based on rhodamine B and its imaging in living cells[J]. Molecules, 2021, 26(11): 3385.
[124] A near-infrared fluorescent probe based on a FRET rhodamine donor linked to a cyanine acceptor for sensitive detection of intracellular pH alternations[J]. Molecules, 2018, 23(10): 2679.
[125] Activity-based fluorescence probes for pathophysiological peroxynitrite fluxes[J]. Coordination Chemistry Reviews, 2022, 454: 214356.
[126] Recent studies focusing on the development of fluorescence probes for zinc ion[J]. Coordination Chemistry Reviews, 2021, 429: 213636.
[127] Fluorescent and luminescent probes for detection of reactive oxygen and nitrogen species[J]. Chemical Society Reviews, 2011, 40(9): 4783-4804.
[128] Organoselenium compounds as fluorescent probes[J]. Coordination Chemistry Reviews, 2015, 300: 86-100.
[129] Fluorogenic probes for disease-relevant enzymes[J]. Chemical Society Reviews, 2019, 48(2): 683-722.
[130] The research progress of organic fluorescent probe applied in food and drinking water detection[J]. Coordination Chemistry Reviews, 2021, 427: 213557.
[131] “Turn-on” fluorescent sensing with “reactive” probes[J]. Chemical communications, 2011, 47(27): 7583-7601.
[132] Small molecular fluorescent probes for the detection of lead, cadmium and mercury ions[J]. Coordination Chemistry Reviews, 2021, 429: 213691.
[133] A general highly efficient synthesis of biocompatible rhodamine dyes and probes for

live-cell multicolor nanoscopy[J]. Nature Communications, 2023, 14(1): 1306.
[134] Molecular probes for fluorescence lifetime imaging[J]. Bioconjugate chemistry, 2015, 26(6): 963-974.
[135] Fluorescent labeling of biomolecules with organic probes[J]. Chemical reviews, 2009, 109(1): 190-212.
[136] Nanomaterial-based activatable imaging probes: from design to biological applications[J]. Chemical Society Reviews, 2015, 44(21): 7855-7880.
[137] Green and red fluorescent dyes for translational applications in imaging and sensing analytes: A dual‐color flag[J]. ChemistryOpen, 2018, 7(1): 9-52.
[138] Photoswitching Emission with Rhodamine Spiroamides for Super‐resolution Fluorescence nanoscopies[J]. Israel Journal of Chemistry, 2013, 53(5): 267-279.
[139] Recent advances in fluorescent probes for lipid droplets[J]. Chemical Communications, 2022, 58(10): 1495-1509.
[140] Intracellular FRET-based probes: a review[J]. Methods and applications in fluorescence, 2015, 3(4): 042006.
[141] Design principles, sensing mechanisms, and applications of highly specific fluorescent probes for HOCl/OCl–[J]. Accounts of chemical research, 2019, 52(8): 2158-2168.
[142] Tuning the pKa of fluorescent rhodamine pH probes through substituent effects[J]. Chemistry–A European Journal, 2017, 23(56): 14064-14072.
[143] Novel rhodamine probe for colorimetric and fluorescent detection of Fe3+ ions in aqueous media with cellular imaging[J]. Spectrochimica Acta Part A: Molecular and Biomolecular Spectroscopy, 2020, 242: 118757.
[144] Fluorescent chemical probes for accurate tumor diagnosis and targeting therapy[J]. Chemical Society Reviews, 2017, 46(8): 2237-2271.
[145] Fluorescent bioimaging of pH: from design to applications[J]. Chemical Society Reviews, 2017, 46(8): 2076-2090.
[146] Degradation of Rhodamine dyes by Advanced Oxidation Processes (AOPs)–Focus on caviatation and photocatalysis-A critical review[J]. Water Resources and Industry, 2023: 100220.
[147] Fluorescent probes for selective determination of trace level Al 3+: recent developments and future prospects[J]. Analytical Methods, 2013, 5(22): 6262-6285.
[148] Fluorescein derivatives as fluorescent probes for pH monitoring along recent biological applications[J]. International journal of molecular sciences, 2020, 21(23): 9217.
[149] Efficient fluorescence resonance energy transfer-based ratiometric fluorescent cellular imaging probe for Zn2+ using a rhodamine spirolactam as a trigger[J]. Analytical chemistry, 2010, 82(8): 3108-3113.
[150] Rhodamine‐based fluorescent turn‐on probe for facile sensing and imaging of ATP in mitochondria[J]. ChemistrySelect, 2017, 2(25): 7654-7658.
[151] Efficient fluorescence resonance energy transfer-based ratiometric fluorescent cellular imaging probe for Zn2+ using a rhodamine spirolactam as a trigger[J]. Analytical chemistry, 2010, 82(8): 3108-3113.
[152] Fluorescent probes for the detection of chemical warfare agents[J]. Chemical Society Reviews, 2023, 52(2): 601-662.

[153] Engineering a novel rhodamine-based fluorescent probe using host-guest interactions for reversible, selective, and sensitive detection of herbicide paraquat[J]. Sensors and Actuators B: Chemical, 2023, 383: 133556.

[154] Progress of synthesis and separation of regioisomerically pure 5 (6)-substituted rhodamine[J]. Current Organic Chemistry, 2016, 20(15): 1584-1590.

[155] Near-infrared fluorescent probes with BODIPY donors and rhodamine and merocyanine acceptors for ratiometric determination of lysosomal pH variance[J]. Sensors and Actuators B: Chemical, 2019, 294: 1-13.

[156] Recent development of synthetic probes for detection of hypochlorous acid/hypochlorite[J]. Spectrochimica Acta Part A: Molecular and Biomolecular Spectroscopy, 2020, 240: 118545.

[157] Recent progress in the design and applications of fluorescence probes containing crown ethers[J]. Chemical Society Reviews, 2017, 46(9): 2437-2458.

[158] Organic fluorescent probes for monitoring autophagy in living cells[J]. Chemical Society Reviews, 2021, 50(1): 102-119.

[159] Activity-based sensing fluorescent probes for iron in biological systems[J]. Current opinion in chemical biology, 2018, 43: 113-118.

[160] Recent advances in the development of responsive probes for selective detection of cysteine[J]. Coordination Chemistry Reviews, 2020, 408: 213182

[161] Environmentally robust rhodamine reporters for probe-based cellular detection of the cancer-linked oxidoreductase hNQO1[J]. ACS Chemical Biology, 2016, 11(1): 231-240

[162] Mitochondrial-targeted fluorescent probes for reactive oxygen species[J]. Current opinion in chemical biology, 2010, 14(1): 50-56.

[163] Recent developments of fluorescent probes for the detection of gasotransmitters (NO, CO and H2S)[J]. Coordination Chemistry Reviews, 2013, 257(15-16): 2335-2347

[164] brilliant red pigment dye-based fluorescent probes and their applications[J]. Chemical Society Reviews, 2015, 44(1): 58-77

[165] Metal-coordinated fluorescent and luminescent probes for reactive oxygen species (ROS) and reactive nitrogen species (RNS)[J]. Coordination Chemistry Reviews, 2021, 427: 213581

[166] Near-infrared fluorescent probes: a next-generation tool for protein-labeling applications[J]. Chemical Science, 2021, 12(10): 3437-3447.

[167] Development of fluorescent probes for bioimaging applications[J]. Proceedings of the Japan Academy, Series B, 2010, 86(8): 837-847.

[168] Reversible fluorescent probes for biological redox states[J]. Angewandte Chemie International Edition, 2016, 55(5): 1602-1613.

[169] Fluorescent and colorimetric probes for detection of thiols[J]. Chemical Society Reviews, 2010, 39(6): 2120-2135.

[170] Recent progress in the two-photon fluorescent probes for metal ions[J]. Coordination Chemistry Reviews, 2021, 427: 213574.

[171] Reaction-based small-molecule fluorescent probes for chemoselective bioimaging[J]. Nature Chemistry, 2012, 4(12): 973-984.